NEOPLASIA
www.neoplasia.com

Volume 20 Number 9 September 2018 pp. 905–916 905

Telomeric Recombination Induced by DNA Damage Results in Telomere Extension and Length Heterogeneity

Haiying Liu[*,†], Yujie Xie[*,†], Zepeng Zhang[*,†], Pingsu Mao[*,†], Jingfan Liu[*,†], Wenbin Ma[*] and Yong Zhao[*,†]

[*]MOE Key Laboratory of Gene Function and Regulation, School of Life Sciences, Sun Yat-sen University, Guangzhou 510006, P. R. China; [†]Collaborative Innovation Center of High Performance Computing, National University of Defense Technology, Changsha 410073, P. R. China

Abstract

About 15% of human cancers counteract telomere loss by alternative lengthening of telomeres (ALT), which is attributed to homologous recombination (HR)–mediated events. But how telomeric HR leads to length elongation is poorly understood. Here, we explore telomere clustering and telomeric HR induced by double-stranded breaks (DSBs). We show that telomere clustering could occur at G1 and S phase of cell cycle and that three types of telomeric HR occur based on the manner of telomeric DNA exchange: equivalent telomeric sister chromatin exchange (T-SCE), inequivalent T-SCE, and No-SCE. While inequivalent T-SCE increases telomere length heterogeneity with no net gain of telomere length, No-SCE, which is presumably induced by interchromatid HR and/or break-induced replication, results in telomere elongation. Accordingly, cells subjected to long-term telomeric DSBs display increased heterogeneity of length and longer telomeres. We also demonstrate that DSBs-induced telomere elongation is telomerase independent. Moreover, telomeric recombination induced by DSBs is associated with formation of ALT-associated PML body and C-circle. Thus, DNA damage triggers recombination mediated elongation, leading to the induction of multiple ALT phenotypes.

Neoplasia (2018) 20, 905–916

Introduction

Approximately 85% of human cancers maintain telomere length by telomerase, whereas the remaining 15% maintain telomere length in an alternative way called alternative lengthening of telomeres (ALT) [1]. ALT cancer cells are characterized by several hallmarks [1,2], including the following: first, the telomere length of ALT cells is heterogeneous, ranging from undetectable to extremely long; second, ALT cells contain ALT-associated promyelocytic leukemia (PML) bodies (APBs), a special form of PML body that includes telomere DNA, whereas PML body is usually unrelated to the telomere in normal human cells and telomerase-positive cancer cells [3,4]; third, abundant extrachromosomal telomeric circle DNA is present in ALT cells, including both double-stranded telomeric circles (t-circles) and partially single-stranded circles (C-circles) [5,6]. In addition, high frequency of telomere sister chromatid exchange (T-SCE) has been specifically detected in ALT cells, consistent with the widely accepted hypothesis that ALT is mediated by homologous recombination (HR)–based mechanism [7,8].

Naturally, spontaneous DNA lesions occur every day in human cells [9]. ALT cells have been reported to have large amounts of intrinsic DNA damages that may cause chromatin instability [10,11]. Accordingly, persistent DNA damage response at telomeres, termed telomere dysfunction-induced foci (TIFs), is often observed in ALT cells but with much less frequency in non-ALT human cells [12,13].

Abbreviations: ALT, Alternative lengthening of telomeres; APBs, ALT-associated PML bodies; BIR, Break-induced replication; CO-FISH, Chromosome orientation fluorescence *in situ* hybridization; DDR, DNA damage response; DOX, Doxycycline; DSBs, Double-strand breaks; HR, Homologous recombination; PML, Promyelocytic leukemia; RTL, Relative telomere length; SD, Standard deviation; T-SCE, Telomeric sister chromatid exchange; TIFs, Telomere dysfunction-induced foci; TRAP, Telomeric repeat amplification protocol; TRF, Telomere restriction fragment.

Address all correspondence to: Yong Zhao, No. 135, Xingang Xi Road, Guangzhou, 510275, P. R. China. E-mail: zhaoy82@mail.sysu.edu.cn

Received 10 May 2018; Revised 20 July 2018; Accepted 24 July 2018

1476-5586
https://doi.org/10.1016/j.neo.2018.07.004

Our previous work and study from de Lange's group found that double-strand breaks (DSBs) in telomeric DNA can be repaired by HR in human and mouse cells [14,15]. It is thus interesting to ask whether intrinsic DNA damages in ALT cells are able to drive HR-mediated telomere elongation.

It has been found that DSBs at ALT telomeres trigger long-range movement and clustering between chromosome termini [16]. Our previous study also demonstrated that artificially induced DSBs at telomeres drive clustering of telomeres in telomerase-positive cells [14]. Considering that all telomeres at chromosome ends have identical DNA sequences (TTAGGG/AATCCC), telomere clustering represents a homology searching mechanism specialized in telomeric DNA that may provide a new approach for recombination between not only sister telomeres but also nonsister telomeres. In this scenario, DSB-induced HR may occur between telomeres of both sister and nonsister chromatids. In addition, DSBs at telomeres may also trigger the mechanism termed break-induced replication (BIR) for repair. Because of telomere clustering, homologous template required by BIR for DNA synthesis can be provided by nonsister telomeres or sister telomeres. In fact, BIR occurring at G1 phase of cell cycle has been identified to contribute to lengthening of telomeres in ALT cells [16–18].

The main purpose of this study is to answer the question of whether telomeric DSB-induced recombination recapitulates telomere elongation observed in ALT cells. To directly address this, we induced telomeric DSBs using the CRISPR/Cas9 system in ALT-negative 293T cells and performed chromosome orientation-FISH (CO-FISH) and quantitative FISH (q-FISH) to calculate relative length of every telomere after recombination. We observed that DSBs-induced telomeric sister chromatid exchange (T-SCE) contributes to telomere length heterogeneity, whereas telomeres were primarily elongated by nonsister chromatid exchange (No-SCE). After a long-term induction of telomeric DSBs, non-ALT 293T cells displayed longer telomeres and heterogonous length distribution, as well as the formation of APBs and high abundance of C-circle DNA, recapitulating features of ALT cells.

Material and Methods

Cell Culture and Long-Term Transfection

The 293T and U2OS cells were originally obtained from American Type Culture Collection (Manassas, VA). Two subtypes of 293T cells bearing different telomere length (5 kb and 15 kb) were used in this work. Unless specifically labeled, 293T cells described in text and figures are 293T 15 kb. Lentivirus with doxycycline (Dox) inducible HA-Cas9 was transfected into 293T and selected with puromycin. The expression of HA-Cas9 was detected with anti-HA antibody (Proteintech); GAPDH was detected as loading control (anti-GPDH, Proteintech). 293T and U2OS cells were grown in Dulbecco's modified Eagle medium (Gibco) supplemented with 10% fetal bovine serum (Hyclone) and 100 U/ml penicillin/streptomycin (Hyclone) at 37°C and 5% CO_2. Plasmids DNA containing sgRNAs (Tel1, Tel2) or control (Scramble) were transfected into 293T-Cas9 by the polyethyleneimine (PEI) method. Briefly, 6 μg DNA was incubated with 18 μl PEI in a total of 480 μl opti-MEM for 15 minutes and then added to cells cultured in 6 cm–diameter culture dish. The medium was exchanged with fresh medium containing doxycycline (0.25 μg/ml) or DMSO (control) after 6 hours of transfection. For long-term transfection, sgRNAs were transfected into cells six times at 7-day intervals before analysis. The guiding sequences (sgRNA) were as follows: Tel 1: 5′-CACCGTTACCGTTAGGGTTAGGGTTA-3′; Tel 2: 5′-CACCGTTAGGGTTAGGGTTAGGGTTA-3′; control: 5′-CACCGGGTCTTC GAGAAGACCTGTTT-3′; Tel1 and Tel2 targeted the telomere, while the control was a scramble sequence.

Telomere Restriction Fragment (TRF) Assay

Genomic DNA was extracted using the AxyPrep Blood Genomic DNA Miniprep Kit (Axygen Biosciences, Union City, CA) following manufacturer's instructions. Genomic DNA was digested by the HinfI, MSPI, and AfaI restriction enzymes at 37°C overnight and resolved on a 0.7% agarose gel. The gel was denatured, dried, and then hybridized with ^{32}P-labeled $(TTAGGG)_4$ oligonucleotides and exposed to a PhosphorImager screen. The weighted mean telomere length was calculated as described previously [19].

Immunofluorescence-FISH (IF-FISH)

Cells were grown on a coverslip, washed with PBS and fixed in 4% paraformaldehyde for 15 minutes at room temperature, and then permeabilized in 0.5% Triton X-100 at room temperature for 30 minutes. The cells were washed thrice with 1× PBST and blocked with 5% goat serum for 1 hour at room temperature. The cells were first incubated with primary antibody (anti-53BP1, Novus Biologicals; anti-PML, Santa Cruz) overnight at 4°C and then with secondary antibody conjugated with DyLight 488 for 1 hour at room temperature. The coverslip was washed with PBST and fixed in 4% paraformaldehyde for 10 minutes, washed in ethanol series solutions, denatured at 85°C for 5 minutes, hybridized with Cy3-labeled CCCTAA PNA probe (Panagene) for 2 hours at 37°C, washed and mounted with DAPI stain, and visualized using a Zeiss microscope.

Chromosome Orientation Fluorescence In Situ Hybridization (CO-FISH)

CO-FISH was performed as previously described with minor modification [20]. Briefly, after 34 hours of last transfection, 293T cells were incubated with BrdU for 14 hours; nocodazole (0.5 μg/ml) was added 3 hours before harvest. For U2OS, cells were incubated with BrdU for 20 or 72 hours; nocodazole (0.5 μg/ml) was added 5 hours before harvest. Cells were trypsinized and resuspended in a hypotonic solution of 0.075 M KCl incubated at 37°C for 30 minutes. The cells were fixed thrice with methanol:acetic acid (3:1) for 10 minutes each time. The cells were then spread onto slides, digested with pepsin (1 mg/ml) for 40 seconds, and exposed to UV (365 nm, UVP-CL1000) in the presence of Hoechst for 35 minutes. The cells were treated with Exo III (100 U for 2 hours at 37°C), hybridized with C-rich (green, FITC-labeled) and G-rich probe (red, Cy3-labeled) in sequence, mounted with DAPI, and observed using a Zeiss microscope.

Determination of Relative Length of Telomeres in CO-FISH

To eliminate the difference between hybridization with C-rich (green) and G-rich (red) probe, the ratio of red to green fluorescence intensity in every karyotype was calculated (total red intensity/total green intensity). The red fluorescence intensity was then normalized by dividing with this ratio, obtaining intensity value that is comparable to the green fluorescence. For telomeres with T-SCE that display both green and red fluorescence, the relative telomere length (RTL) was calculated as the sum of green and normalized red fluorescence intensity.

Telomere Quantitative-FISH (q-FISH)

Cells were treated with 0.5 μg/ml nocodazole for 3 hours to enrich cells at metaphase. Cells were harvested and q-FISH was performed as previously described [21]. Cy3-labeled $(CCCTAA)_3$ PNA probe was used. Images were taken using a Zeiss microscope. The fluorescence intensity of the telomeres was analyzed by Axio Vision software 4.8 and the TFL-TELO program.

Constant-Field Gel Electrophoresis (CFGE)

CFGE was performed as described previously [14]. Cells were imbedded in 0.7% agarose, lysed with 0.5% SDS in Tris-HCl, and digested with RNase A (100 μg/ml) and proteinase K (250 μg/ml) at 37°C overnight. Gel electrophoresis was performed using 0.7% agarose in TAE buffer. In-gel hybridization analysis of telomeric DNA was performed as follows: the gel was dried for 1 hour at room temperature and hybridized overnight at 42°C with a telomeric probe in 1× hybridization buffer (2 μg/ml sonicated *Escherichia coli* DNA, 10× Denhards' buffer, 0.5% SDS, and 5× SSC). The gel was washed four times in wash buffer (2× SSC, 0.5% SDS) and exposed to a PhosphorImager screen (GE Healthcare Life Science).

C-Circle Assay

The C-circle assay was performed as described previously with minor modification [5]. Briefly, genomic DNA was digested with the HinfI, MSPI and AfaI restriction enzymes and RNase A (Fermentas) at 37°C overnight. A total of 20 ng digested DNA was used for amplification with Φ29 DNA polymerase (NEB) at 30°C for 8 hours followed by 65°C for 20 minutes. The products were blotted onto nitrocellulose filter membrane, UV cross linked, and hybridized with ^{32}P-labeled C-probe. The membrane was then exposed to phosphor screen and scanned. The signals were quantified using ImageQuant software.

Telomeric Repeat Amplification Protocol (TRAP) Assay

The PCR-based TRAP assay was performed as described previously [22]. Cells were counted, pelleted, and resuspended in 1× CHAPS lysis buffer and incubated on ice for 30 minutes. The supernatant was collected after centrifugation and diluted into volume in which 1 μl lysate was equal to 500 cells. One microliter of lysate was used for extension; the lysate heated at 85°C for 10 minutes was used as a heating control and ddH_2O as a negative control. The products were separated in 8% polyacrylamide gel at 250 V for 2 hours, stained with gel red for 15 minutes, and visualized under UV illumination.

EdU Staining and Detection of Telomere Clustering

Tel2 and scramble sgRNAs were transfected into 293T-Cas9 cells cultured in Dox-containing medium. After 24 hours of transfection, 5-ethynyl-2-deoxyuridine (EdU, 50 μM) was added to medium and incubated for 10 minutes. Cells were fixed and permeabilized as mentioned in IF-FISH assay. The cells were hybridized with Cy3-labeled CCCTAA PNA probe (Panagene) for 2 hours at 37°C and stained with freshly prepared staining solution (10 μM fluorescent azide, 1 mM CuSO4, and 10 mM ascorbic acid dissolved in PBS) for 10 minutes to visualize EdU. The coverslip was mounted with DAPI and visualized using a Zeiss microscope. The average diameter of telomere spots in normal 293T cells was ~2 pixels. The telomere clustering is defined as telomere signals with diameters bigger than 4 pixels, and cells with more than 4 clustered telomere foci were quantified for each group.

Statistical Analysis

The Student's 2-tailed unpaired *t* test was used to determine statistical significance. The resulting *P* values are indicated in the figures.

Results

Inducible CRISPR/Cas9 System for Generation of Sustained Telomeric DSBs

To specifically generate double-strand breaks in telomeric DNA, we used the CRISPR/Cas9 system, which consists of the Cas9 enzyme and sgRNA-targeting telomeric sequences. In this study, the doxycycline-inducible Cas9 enzyme was stably expressed in human non-ALT 293T cells, termed 293T-Cas9. The sgRNAs targeting telomeric sequence (Tel1, Tel2) or scramble sequence (Ctl) were transfected into 293T-Cas9 cells. When doxycycline (Dox) was added to culture medium, the Cas9 enzyme was successfully expressed (Figure 1*A*). CRISPR/Cas9-induced telomeric DSBs were verified by constant-field gel electrophoresis (CFGE) followed by hybridization under native condition with a C-rich telomere-specific probe. While intact genomic DNA stays in the plug, the amount of DNA released into the gel as linear DNA fragments is proportional to the number of DSBs in the genome; telomeric probe identifies the fraction of DNA fragments derived from CRISPR/Cas9-cleaved telomeres. The result showed that co-expressed Cas9 and Tel1 or Tel2 induced the release of telomeric fragments from the genome, whereas the expression of Tel1 or Tel2 alone (without Dox) or the co-expression of Cas9 and scramble sgRNA (Ctl) did not (Figure 1*B*). (In the following text, Dox is added if not specified). In addition, immunofluorescence (IF) and fluorescence *in situ* hybridization (FISH) were performed to visualize the localization of 53BP1, an indicator of DNA damage response, at telomeres. The colocalization of 53BP1 foci with telomeric DNA was observed in cells coexpressing Cas9 and sgRNA Tel1 or Tel2, but not in cells expressing Cas9 only or coexpressing Cas9 and scramble sgRNA (Ctl) (Figure 1*C-E*).

To explore the long-term effect of telomeric DSBs, 293T-Cas9 cells were consistently treated with Dox and transfected with sgRNAs at 7-day intervals for 6 weeks. In accordance with the previous report that telomeric DSBs are repairable leading to no cell senescence and apoptosis [14], we found that long-term induction of telomeric DSBs has a very limited effect on cell proliferation (Supplementary Figure S1).

Telomere Clustering at G1 or S Phase of Cell Cycle upon Telomeric DSBs

Previously, we observed the phenomenon termed "telomere clustering" when telomeric DSBs were introduced in 293T cells, implying a potential HR between telomeres [14]. To further understand when telomere clustering occurs during cell cycle, 293T-Cas9 cells were incubated with EdU for 10 minutes after sgRNA transfection and subjected to fluorescent azide staining and FISH to visualize EdU and telomeres, respectively (Figure 2*A*). The EdU-positive are cells at S phase of cell cycle, whereas the EdU-negative are cells mostly at G1 phase [23]. The result showed that transfection with Tel2 sgRNA resulted in slight increase (not significant) of EdU-positive cells, demonstrating a limited effect of telomeric DSBs on cell proliferation (Figure 2, *B* and *C*). Cells with clustered telomeres are characterized by increased size (>4 pixels versus <2 pixels) and decreased number of telomeric foci in cell. Based on these standards, cells with clustered telomeres were calculated and

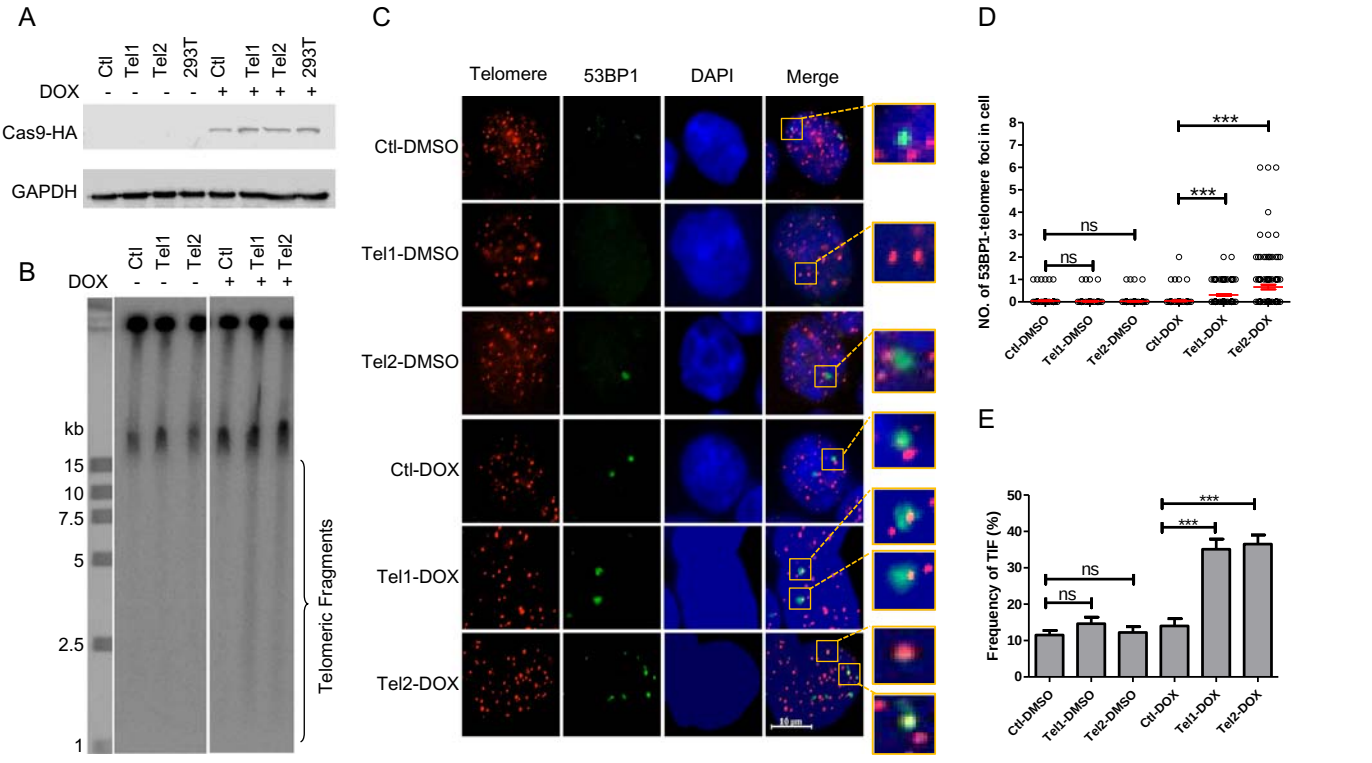

Figure 1. Artificial DSBs at telomeric DNA generated by Cas9. (A) Inducible Cas9 expression in 293T cells. The 293T-Cas9 cells were transfected with the indicated sgRNAs (Ctl: scramble, Tel1 and Tel2: telomere) in the presence or absence of Dox. HA-tagged Cas9 was detected by Western blot 48 hours after transfection (anti-HA, Proteintech). (B) Telomere fragments were generated by the CRISPR/Cas9 system. Cells were treated the same as (A) and analyzed by constant-field gel electrophoresis (CFGE). (C) TIFs were generated by the CRISPR/Cas9 system. Cells were treated the same as in (A). DNA damage response and telomeres were visualized using antibody against 53BP1 (IF) or a probe to telomeric sequences (FISH), respectively. Arrows indicate merged foci. Scale bar, 10 μm. (D) Quantification of foci in panel (C). The number of cells with 1 or more 53BP1 foci was counted, and the percentage of 53BP1 foci colocalized with telomeres per cell was calculated. (E) Quantification of panel (C). The cell with more than one TIF was counted. The percentage of cells with TIF was calculated. All values are mean ± SD of three independent experiments ($n \geq 100$, ***$P < .001$).

classified according to EdU staining. Our results showed: 1) the percentage of cells with clustered telomeres increased upon telomeric DSBs; 2) among these cells, 19% are in G1 phase (EdU negative) and 30% in S phase (EdU positive) (Figure 2, *B* and *D*). These results suggested that DSB-induced telomere clustering could occur at both S and G1 phase of cell cycle.

Telomere Elongation induced by Repair of Telomeric DSBs

In our previous work, we found that telomeric DSBs are repaired by an HR-mediated process [14]. HR in telomeric DNA leads to T-SCE, which can be observed by CO-FISH [24]. In CO-FISH assay, normal telomeres display either a red (leading daughter) or a green signal (lagging daughter) on metaphase spread, whereas telomere with SCE is visualized as a yellow spot merged by red and green signals. As expected, the induction of telomeric DSBs in 293T-Cas9/Tel1 or 293T-Cas9/Tel2 cells led to increased frequency of T-SCEs compared to control cells (293T-Cas9/scramble-sgRNA) (Figure 3, *A* and *B*), demonstrating that telomeric DSBs induced HR-mediated repair at telomeres.

To explore how telomeric HR alters the length of targeted telomeres, the RTL of telomeres with T-SCE was quantified and compared with the mean RTL of telomeres without T-SCEs. To eliminate the effect of different hybridization efficiency between C-rich (green) and G-rich probe (red), the signal intensities from sister chromosomes (green or red) were compared, and the ratio of red to green was calculated. The intensity of red was then converted into the equivalence of green by normalizing with obtained ratio. The signal intensity of the yellow spot was quantified by totaling the red and green signal at the corresponding end of the chromosome. Our results showed that, in most of calculated karyotypes (25/29), the telomeres with T-SCE had a significantly greater average length than telomeres without T-SCE. Figure 3*C* showed six representative karyotypes. Collectively, 288 telomeres with T-SCE from 29 metaphase spreads demonstrated longer average telomere length than telomeres without T-SCE (Figure 3*D*).

We also performed CO-FISH assay on human U2OS cell line, a typical ALT cancer cell line with high frequency of T-SCE [8]. Similar to that observed in 293T-Cas9/Tel, the average telomere length of telomeres with T-SCE (yellow spot) (Supplementary Figure S2*A*) is much longer than those without T-SCE in most of the single karyotype (Supplementary Figure S2*B*) and in total (35 karyotypes) (Supplementary Figure S2*C*).

To exclude the possibility that T-SCE may preferentially occur at long telomeres, two subtypes of 293T cells bearing long and short telomeres (15 kb vs 5 kb) were transfected with CRISPR/Cas9 and Tel2 sgRNA under identical conditions, and resulting T-SCEs were determined by CO-FISH. Our results showed that two cell subtypes (293T-15k and 293T-5k) displayed similar frequencies of T-SCE,

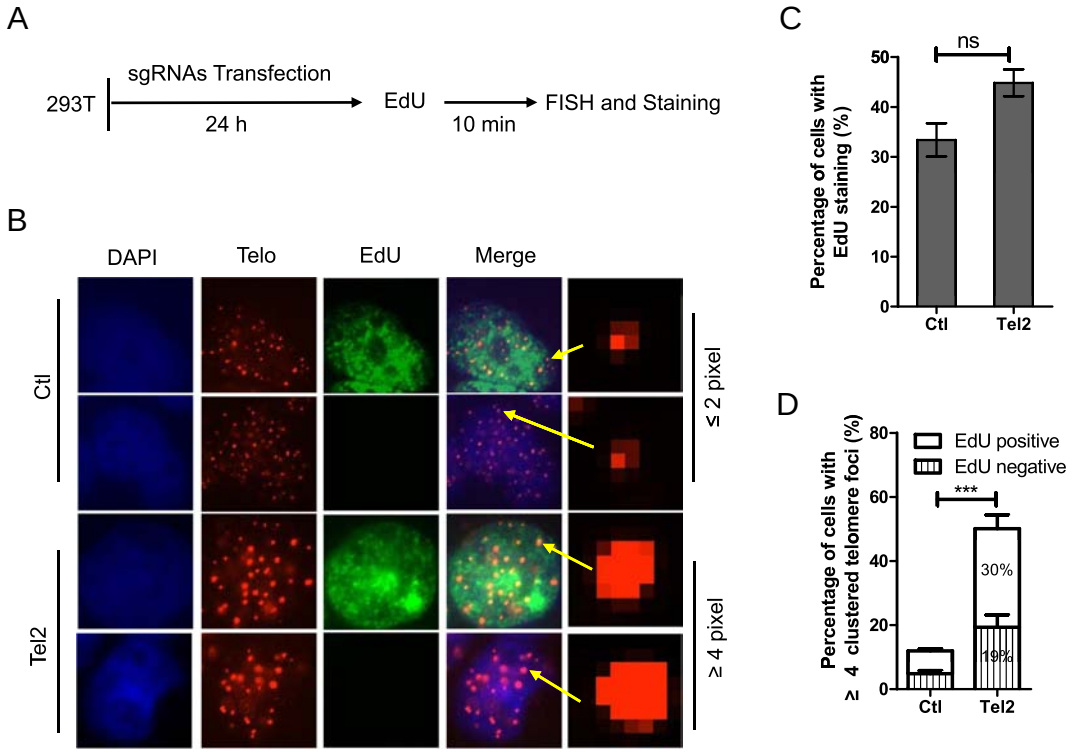

Figure 2. Telomere-clustering upon DSBs at telomeres in both G1 and S phase of cell cycle. (A) Schematic diagram of cell treatment. After 24 hours of sgRNAs transfection, cells were treated with EdU for 10 minutes and subjected to visualization of EdU and telomeres. (B) Clustered telomeres were observed in both EdU-negative (G1) and -positive (S phase) cells. EdU and telomeres were visualized using fluorescent azide staining and telomere probe, respectively. The average size of telomere spots were 2 pixels, and telomere spots with diameters bigger than 4 pixels were defined as clustered telomeres. (C) Quantification of EdU-positive cells in panel (B). (D) Quantification of cells with more than 4 clustered telomere foci in panel (B). More than 845 cells were counted. All values are average ±SD of three independent experiments (***P<.001).

suggesting that telomere length is not a determinant for recombination in our experiment system (Supplementary Figure S3).

Telomere Elongation Primarily Contributed by No-SCE

Yellow spots observed at the ends of chromosome can be classified as follows: unpaired yellow spots (yellow spot at only one chromatid termed No-SCE), paired yellow spots with similar intensity at two sister chromatids (equivalent T-SCE), and paired yellow spots with different intensity at two sister chromatids (inequivalent T-SCE) (Figure 4*A*). Strikingly, a significant number of No-SCE were detected in 293T-Cas9/Tel (both Tel1 and Tel2) and U2OS cells (46.5% and 53.9%, respectively), whereas the frequency of equivalent T-SCE was relatively low (18.1% and 16.8%) (Figure 4*B*).

We then examined the relative length of telomeres with three different recombination events (No-SCE, equivalent T-SCE, and inequivalent T-SCE). In 293T-Cas9/Tel1 and Tel2 cells, the telomeres with No-SCE showed significantly longer length than the average (P<.001), whereas the telomeres with equivalent T-SCE and inequivalent T-SCE have similar telomere length to the average (P= .09 or P=.054, respectively) (Figure 4*C*). Inequivalent T-SCE might be due to repetitive nature of telomeric DNA so that homologous searching and recombination could occur along telomeres (Figure 4*D*). Theoretically, two types of T-SCE would result in no net increase of telomeres, but inequivalent T-SCE may induce telomeres with varying lengths, contributing to heterogeneity of telomere length.

Telomeric No-SCE has been previously reported by several groups in telomerase positive and ALT cells [14,16]. The easiest interpretation is that telomeric recombination between nonsister chromatid may occur (interchromatin recombination). However, interchromatin recombination would not result in net increase of telomere length. There must be other events that could lead to elongation of telomeres.

It has been reported that BIR leads to elongation of telomeres [18]. For BIR, both strands of telomeric DNA are newly synthesized that would be labeled by BrdU during CO-FISH experiment (Supplementary Figure S4*A*). Because Exo III is 3'→5' exodeoxyribonuclease with high specificity for double-stranded DNA [25], it stops digestion as long as single-stranded DNA is generated. Therefore, Exo III digestion would generate intermittent single-stranded G-rich and C-rich DNA, which could hybridize with C-rich (green) or G-rich probe (red) under native conditions, forming yellow foci (Supplementary Figure S4*B*). To verify this experimentally, U2OS cells were treated with BrdU for 72 hours (approximately three population doublings) so that most of telomeres are BrdU labeled at both strands of DNA (G-rich and C-rich). As expected, we observed that ~70% of telomeres are yellow when these cells were subjected to CO-FISH (Supplementary Figure S4*C*).

We also tested telomeric recombination in U2OS cells. Surprisingly, all telomeres with three recombination events (No-SCE, equivalent T-SCE, and inequivalent T-SCE) showed longer telomere length than the average (Supplementary Figure S5), implying that

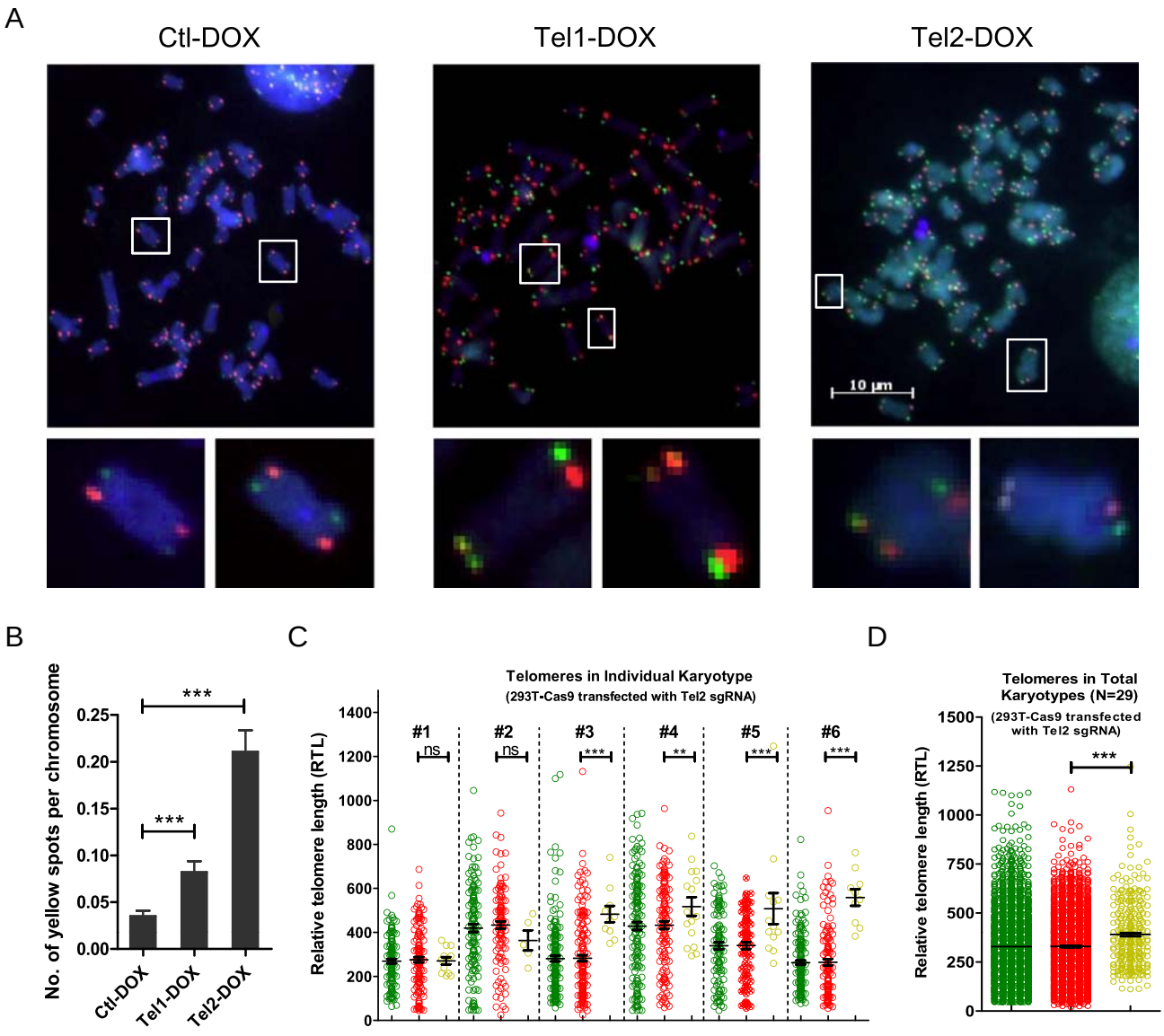

Figure 3. HR mediated repair of telomeric DSBs leads to lengthening of telomeres. (A) T-SCE was induced by telomeric DSBs. 293T-Cas9 cells were transfected with the indicated sgRNAs. Cells were transfected six times at 7-day intervals in the presence of Dox. T-SCE was visualized by CO-FISH (yellow spots). Scale bar, 10 μm. (B) Quantification of T-SCE from panel (A). Frequencies of yellow spots (indicating T-SCE) were counted. All values are mean ± SD of three independent experiments (n>30 karyotypes, ***P<.001). (C) The RTL in panel (A) was quantified (293T-Cas9 + Tel2). Six representative karyotypes were shown. RTL of telomeres with green, red, or yellow color was calculated. (D) Telomeres with T-SCE were longer than telomeres without T-SCE (293T-15 kb + Tel2-Dox). All values are mean ± SD of three independent experiments; 288 instances of T-SCE in 29 karyotypes were quantified (***P<.001).

besides telomeric HR or BIR, additional elongation of telomeres might occur [1]. Nevertheless, telomeres with No-SCE showed the longest length in 293T-Cas9/Tel and U2OS, suggesting that No-SCE, which is presumably induced by BIR, makes a contribution to telomere elongation.

Increased Length Heterogeneity of Telomeres after Exposure of Cells to Substained Telomeric DSBs

As a result of No-SCE and inequivalent T-SCE, it is expected that sustained DSBs at telomeres may not only elongate telomeres but also change their length heterogeneity. To test it, q-FISH was performed to determine the RTL. In 293T-Cas9 cells transfected with scramble sgRNA (Ctl-DOX), telomere length was relatively homogenous at a single cell and population level (Figure 5, *A-C*). However, in cells transfected with Tel1 or Tel2 (Tel1-DOX or Tel2-DOX), telomere length displayed a heterogeneous distribution (Figure 5, *A-C*). In addition, we observed increased average length of telomeres in Tel1 or Tel2-transfected cells compared to scramble sgRNA transfected cells (Ctl-DOX) (Figure 5*C*).

Telomerase-independent telomere elongation induced by sustained DSBs at telomeres

After 293T-Cas9 cells were exposed to sustained telomeric DSBs for 6 weeks, their telomere length was assayed by TRF. We observed that in the presence of dox induction, 293T-Cas9 cells transfected with Tel1 or Tel2 sgRNAs bear longer telomeres than cells transfected

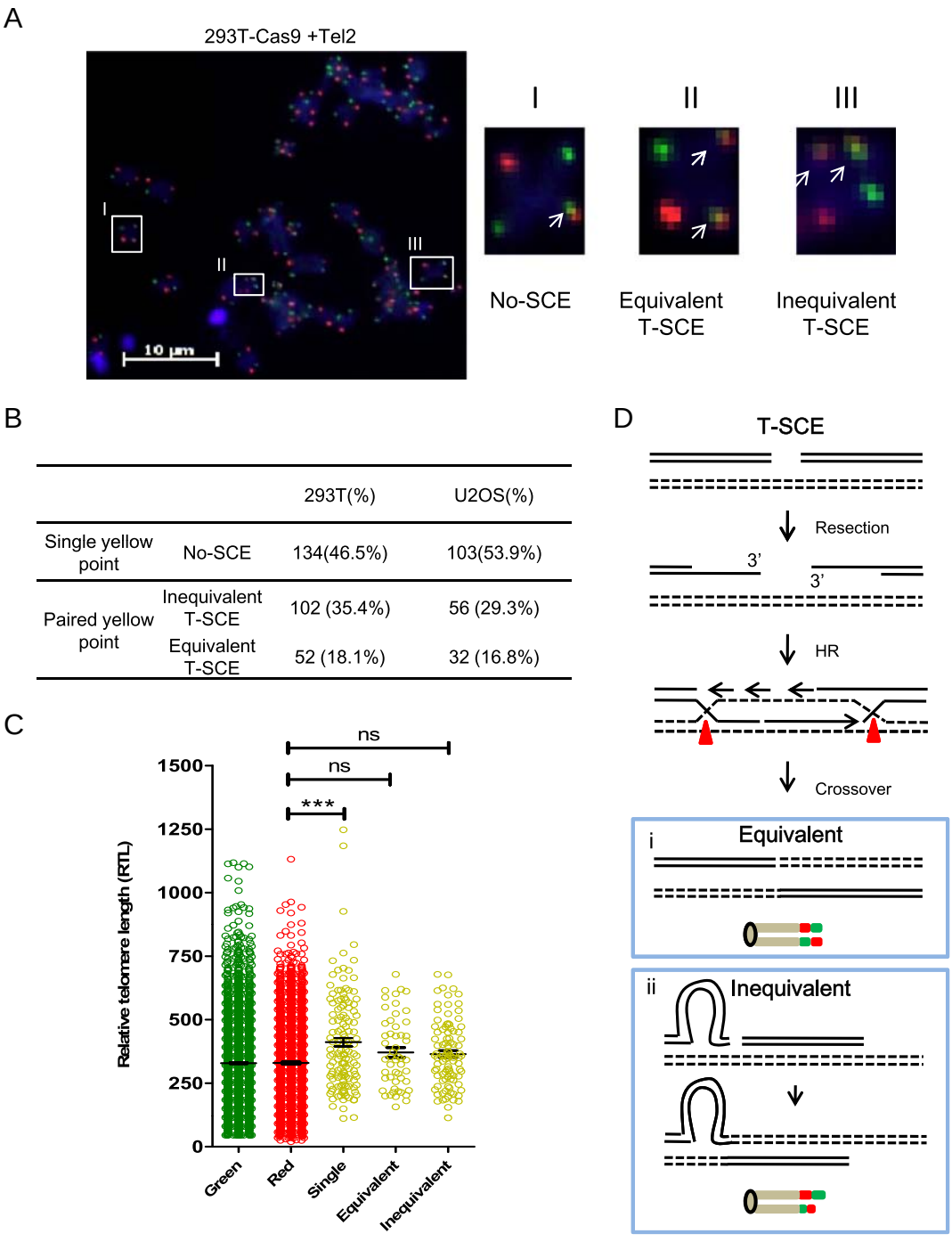

Figure 4. No-SCE contributes to the lengthening of targeted telomeres. (A) Three types of SCE in a representative karyotype (I. No-SCE; II. equivalent T-SCE; III. inequivalent T-SCE). (B) Occurrence frequencies of three types of SCE in 293T-Cas9/Tel (sum of Tel1 and Tel2 with Dox) and U2OS cells. Karyotypes in three independent experiments were calculated. (C) Relative length of telomeres with No-SCE, equivalent T-SCE, or inequivalent T-SCE in 293T-Cas9/Tel cells. Telomeres without SCE (red or green) were used as control. Twenty-nine karyotypes were calculated. All values are mean ± SD of three independent experiments (***P<.001, ns: not significant). (D) Schematic diagram of T-SCE (equivalent and inequivalent) caused by HR.

with scramble sgRNA (Figure 6, *A* and *B*). Telomere elongation was not observed when cells were transfected with telomeric sgRNAs without dox induction (Figure 6*A*), excluding the possibility that sgRNAs might be involved in telomere length elongation. We also performed the TRAP assay to determine telomerase activity in transfected and control cells. No obvious difference was observed for all cells tested (Figure 6*C*), suggesting that the lengthened telomere is not due to increased telomerase activity.

It has been reported that DSB induces the activation of ATM or ATR that recruits telomerase to break sites [26]. Our previous work also showed that telomerase preferentially extends the shortest telomeres when telomeres are under nonequilibruim conditions [27]. To exclude

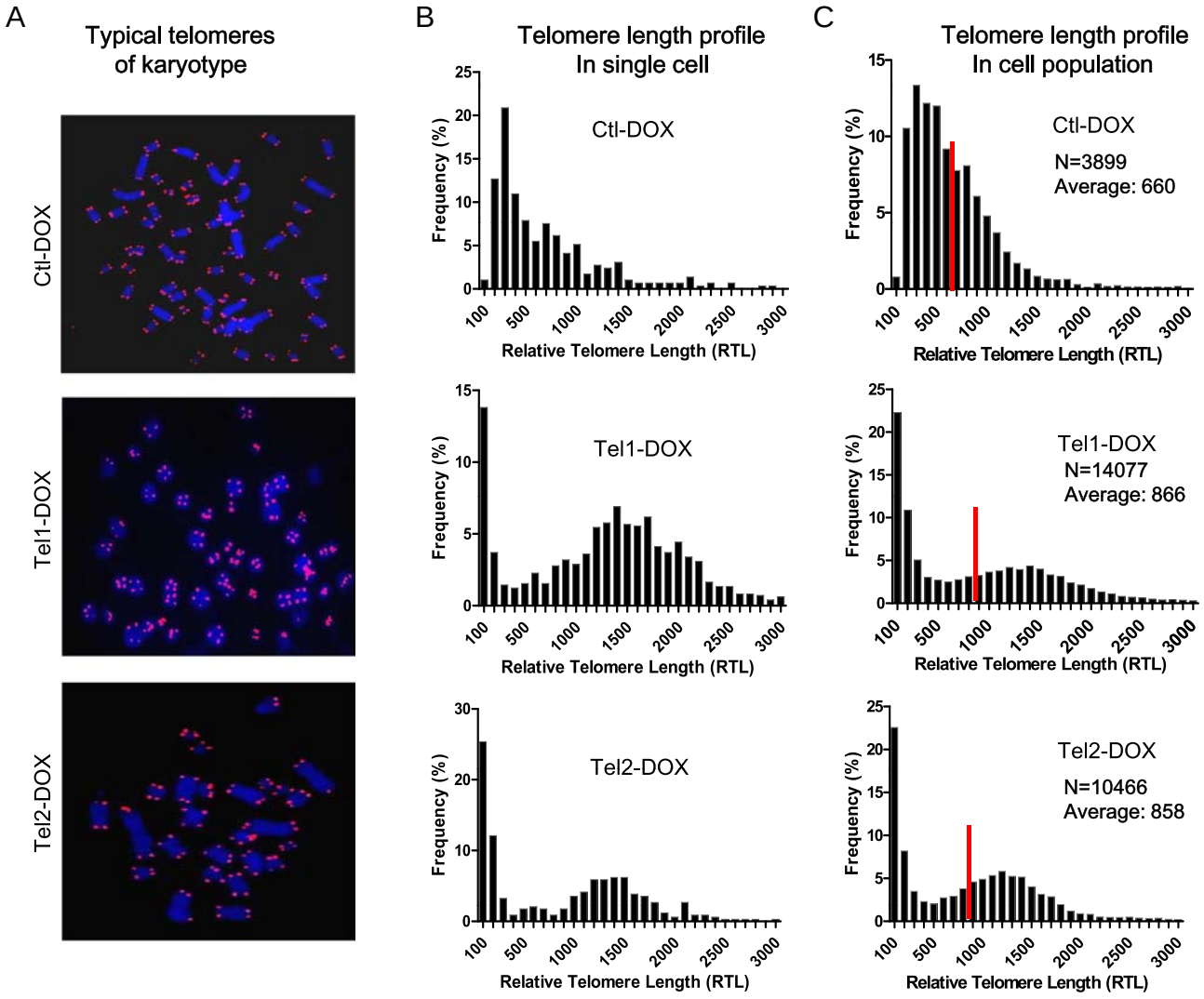

Figure 5. Sustained induction of telomeric DSBs induces heterogeneous telomeres. (A) Representative q-FISH images showing telomeres in Dox induced 293T-Cas9/Tel1 (Tel1-Dox) or Tel2 (Tel2-Dox) and 293T-Cas9/Scramble (Ctl-Dox) cells. SgRNAs were transfected into cells six times at 7-day intervals before analysis. (B) RTL of corresponding single cell in panel (A). (C) RTL of indicated cell populations with Dox. Number of telomeres analyzed (N) is indicated in figures. Red bar indicates the average length of telomeres.

the possibility that telomere elongation might be caused by telomerase extending the broken telomeres, we repeated the above experiment in the presence of BIBR1532, a specific inhibitor of telomerase [28]. As expected, 100 nM of BIBR1532 was able to completely inhibit telomerase activity in 293T-Cas9 cells (Figure 6*D*). For long-term treatment, 10 μM of BIBR1532 was used for 6 weeks that induced significant telomere shortening (Figure 6*E* Ctl lanes). However, sustained expression of telomeric sgRNA (Tel2) restored telomere length (Figure 6*E*), demonstrating telomerase-independent elongation of telomeres.

In the presence of BIBR1532, scramble (Ctl) and Tel2 sgRNA-transfected cells displayed similar proliferation rates, excluding the possibility that different telomere length is due to different division times when telomerase activity is inhibited (Supplementary Figure S6).

Formation of APB and C-Circle upon Sustained Telomeric DSBs

Human ALT cancer cells are also characterized by the presence of extrachromosomal C-circle DNA and ALT-associated promyelocytic leukemia (PML) bodies (APBs) [3,5]. To test whether the long-term induction of telomeric DSBs can recapitulate these hallmarks, the C-circle assay [5] and IF/FISH were performed to determine the abundance of C-circle and formation of APBs, respectively. The amount of C-circle significantly increased when 293T-Cas9 cells were transfected with Tel1 or Tel2 sgRNAs but not with scramble sgRNA (Ctl) (Figure 7, *A* and *B*). Moreover, we found that the average number of PML bodies in cells increased after sustained induction of telomeric DSBs (6 weeks), and the percentage of cells with PML or APBs increased significantly (Figure 7, *C* and *D*).

Discussion

In normal human cells and telomerase-positive cancer cells, telomeric HR is constitutively suppressed, whereas a high frequency of HR was observed at telomeres in ALT cancer cells. It has been widely accepted that the alternative lengthening of telomeres is mediated by telomeric HR [7]. ALT cancer is also characterized by persistent DNA damage response (DDR), i.e., TIF at the telomeres [12,13]. To mimic this

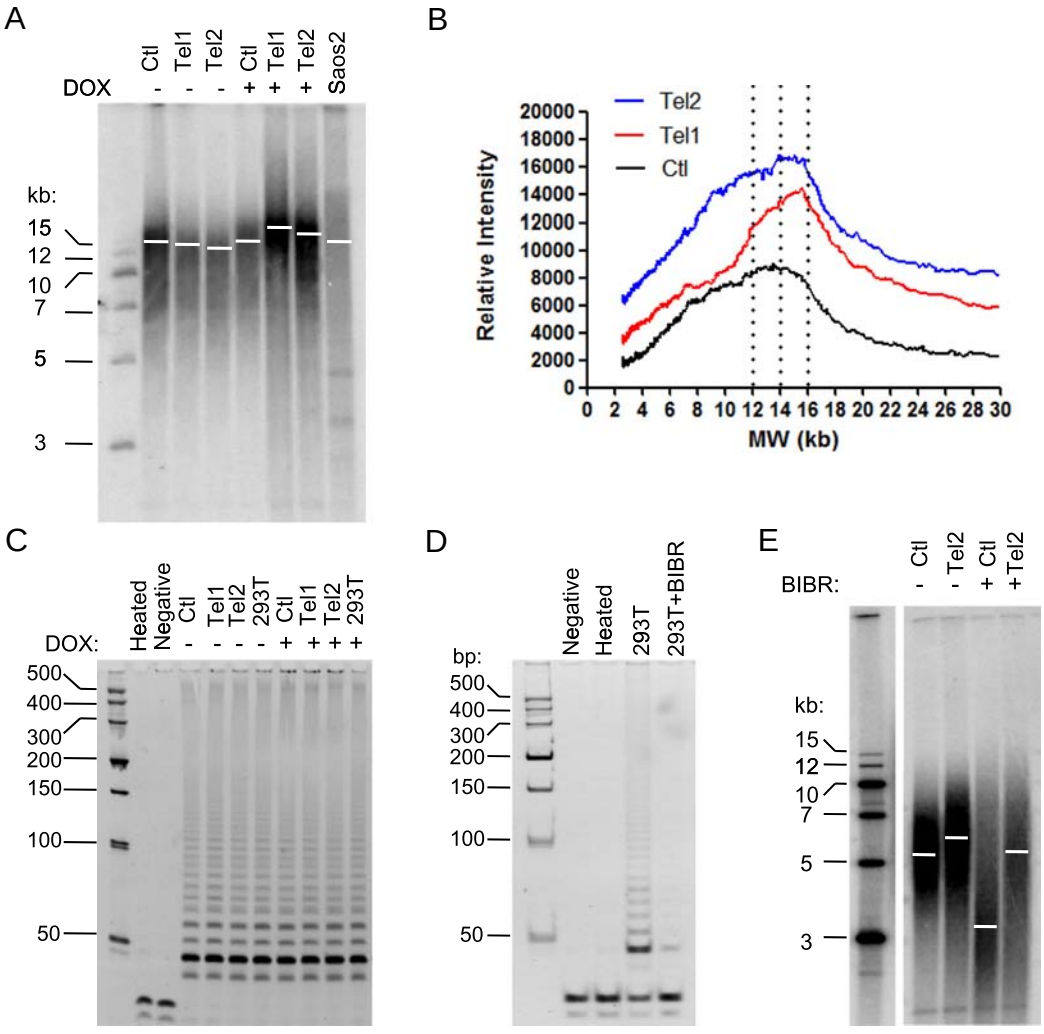

Figure 6. Telomerase independent lengthening of telomeres in cells with sustained telomeric DSBs. (A) Telomeres were lengthened after consistent induction of telomeric DSBs (6 weeks in 293T-15 kb cells). 293T-Cas9 cells were transfected with indicated sgRNAs in the presence or absence of Dox. Telomere length was assayed by TRF. The average length of corresponding cells was indicated by white bar. (B) Quantification of panel (A) (Image J) showing telomere length distribution in scramble sgRNA (Ctl), Tel1, and Tel2 transfected cells with Dox. (C) Unchanged telomerase activity upon sgRNAs transfection. Telomerase activity of cells with indicated sgRNAs was determined by TRAP assay. (D) BIBR1532 inhibits telomerase activity. 293T cell lysate was treated with or without 100 nM BIBR 1532, and telomerase activity was detected by TRAP assay. (E) Telomere elongation in the presence of BIBR 1532 (in 293T-5 kb cells). Indicated cells were treated with or without 10 μM BIBR1532 for 6 weeks; telomere length was then assayed by TRF. The average length of corresponding cells was indicated by white bar.

situation in non-ALT cells, telomeric DSBs were continuously introduced in human 293T cells by inducible CRISPR/Cas9 system. Consistent with our previous findings, we observed telomere clustering and increased frequency of T-SCE (Figures 2*D* and 3*B*), demonstrating the occurrence of HR at telomeres. Theoretically, conventional HR-induced T-SCE would not induce a net increase of telomere length. Indeed, telomeres with T-SCE (equivalent T-SCE and inequivalent T-SCE) have similar lengths with telomeres without T-SCE (Figure 4*C*). Unexpectedly, we also detected a significant number of No-SCE (46.5%) that is likely induced by interchromatin HR or BIR in telomere DNA. Because telomeres with No-SCE show longer length than the rest of telomeres, we proposed that No-SCE is primarily induced by BIR rather than interchromatin HR. Thus, these results support the hypothesis that No-SCE induced by telomeric DSBs contributes to telomere lengthening. Consistently, the long-term exposure of cells to telomeric DSBs led to elongation of telomeres independent of telomerase (Figure 6, *A* and *E*).

BIR is an important pathway specializing in repair of one-ended DSBs, which typically arises at collapsed replication forks or at eroded telomeres [29]. BIR is homology-directed DNA repair that utilizes homologous sequence as a template for DNA synthesis. Our results showed that telomeres underwent clustering in response to DSBs at telomeres (Figure 2*B*). Clustering telomeres thus provide homologous sequence for initiation of BIR. More importantly, the phenomenon of telomere-clustering has been observed at both G1 and S phase of cell cycle, implying that BIR could occur not only within replicated telomeres, i.e., sister chromatid during S phase, but also between nonsister chromatids (G1). This is consistent with the previous finding that BIR at telomeres was detected during G1 phase of cell cycle that contributes to extension of telomeres in ALT cells [18].

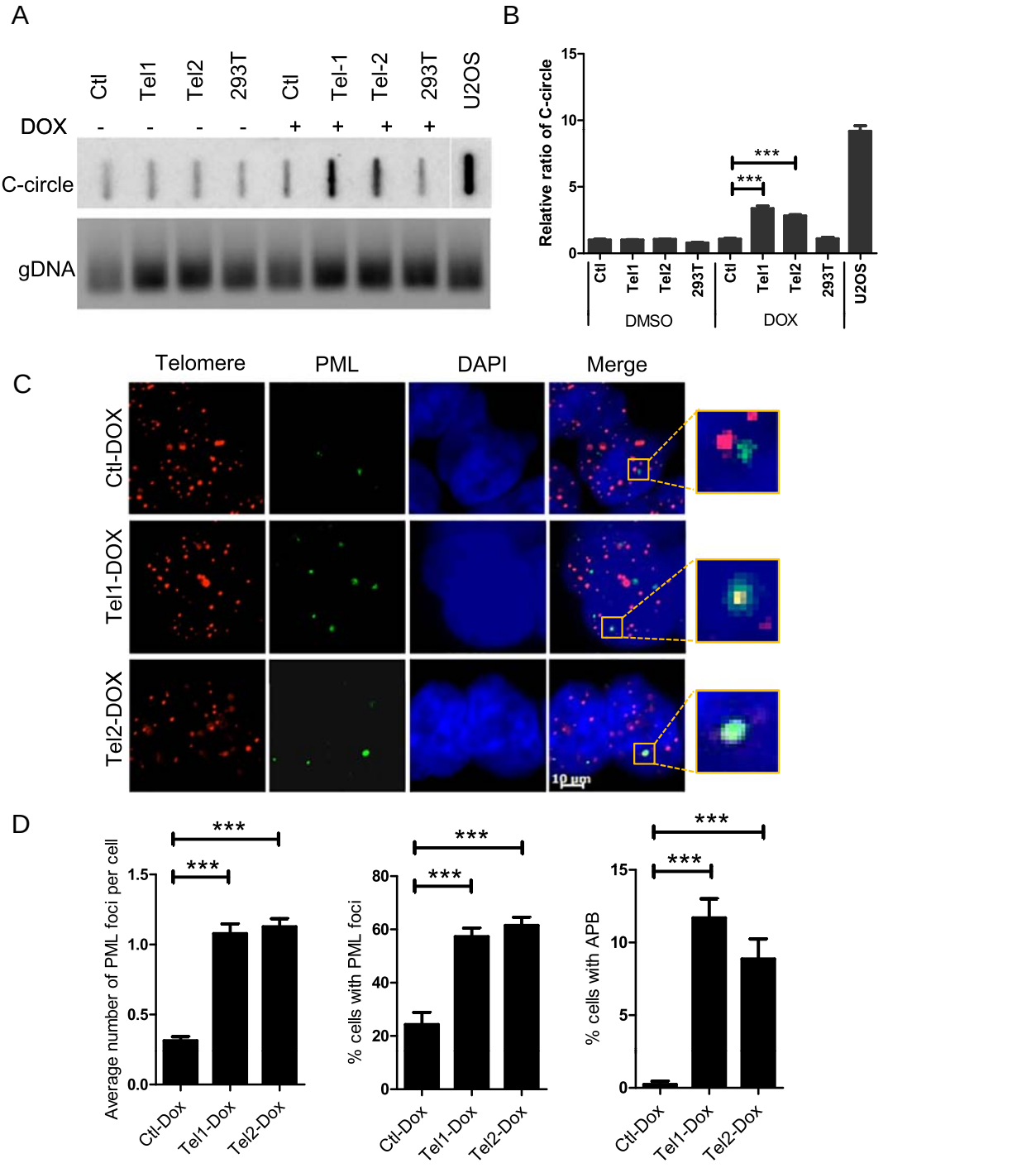

Figure 7. Sustained telomeric DSBs induce the accumulation of C-circle and APBs. (A) C-circle was increased in cells treated with sustained telomeric DSBs. Genomic DNA of indicated cells was extracted, and the abundance of C-circle DNA was determined by C-circle assay. The same amount of genomic DNA was used for the assay (down panel). (B) Quantification of panel (A). All values are mean ± SD of three independent experiments (***P<.001). (C) APBs formation upon sustained telomeric DSBs. APBs in indicated cells were visualized by hybridization using antibody to PML (IF) and telomeric probe (FISH). Arrows indicate merged foci. Scale bar, 10 μm. (D) Quantification of panel (C). The average number of PML foci per cell and the percentage of PML foci or APBs positive cells were calculated. All values are mean ± SD of three independent experiments ($n \geq 100$ for each experiment, ***P<.001).

In addition to telomerase independent lengthening, ALT cells are also characterized by high heterogeneity of telomere length. Because telomeric DNA consists of repetitive sequences, homologous searching and recombination could occur anywhere along telomeres. This would generate inequivalent T-SCE that produce asymmetrical telomeres with one telomere longer/shorter than another. Therefore, telomeres with different length accumulated, leading to heterogeneous distribution of telomere length. In addition, we also observed

the accumulation of short telomeres in cells exposed to repeated telomeric DSBs (Figure 5). Similarly, short telomeres or chromosomes with telomere-free ends are often observed in ALT cancer cells [30]. These telomeres may be caused by inequivalent T-SCE and/or the failure in repairing DSBs at telomeres or by alt-NHEJ mediated repair that induces the loss of telomeric DNA [14,15].

It has been reported that C-circle like structure t-circle-tail DNA is produced during resolution of replication fork stalling at telomeres [31] and that APBs are formed in cell cycle dependent manner during S phase when telomeres are replicated [32]. We observed the C-circle DNA and the formation of APBs in cells with telomeric DSBs (Figure 7). In this scenario, telomeric DSBs may cause replication fork stalling or collapse when encountering telomere replication, and telomeric HR or BIR is activated to resolve stalled replication forks [18,33,34]. How C-circle and APBs coordinate with telomeric HR or BIR to resolve replication stress remains for further investigation.

It should be noted that in addition to HR between sister chromatids (T-SCE) and nonsister chromatids (non-SCE), the recombination between telomere and extrachromosomal circular DNA and/or rolling circle replication-mediated elongation may also occur when DSBs are induced in telomeric DNA, which could contribute to telomere lengthening and length heterogeneity [16]. Moreover, it has been proposed that multiple mechanisms of alternative lengthening may exist in telomerase-negative ALT cell lines [1]. Our results showed that in 293T cells, HR-induced T-SCE (equivalent and inequivalent T-SCE) led to no elongation of targeted telomeres (Figure 4*C*); however, telomeres with T-SCE (equivalent and inequivalent T-SCE) in telomerase-negative U2OS cells are longer than telomeres without T-SCE (Supplementary Figure S5*B*), indicating an additional extension mechanism existing in U2OS cells.

There is persistent DDR at telomeres in ALT cancer cells that may serve as a consistent trigger for ALT. It is thus hypothesized that decrease of telomeric DNA damages or block of telomeric DDR would attenuate ALT activity. In supporting this, it has been found that the inhibition of ATR, a crucial DDR protein for signal transduction, induces cell death of ALT cancer [35]. Furthermore, the increase of DNA damage at telomeres enhances ALT activity [16]. The present study provides a new insight into understanding of mechanisms underlying ALT and may facilitate development of effective ALT-targeted anticancer therapies.

Acknowledgements

We thank all the members in Dr Zhao's laboratory for insightful scientific discussion. We thank Dr. Qin Xiaofeng at the Center of Systems Medicine, Institute of Basic Medical Sciences, Chinese Academy of Medical Sciences, and Peking Union Medical College, for providing 293T cells.

Funding

This work was supported by the National Natural Science Foundation of China grants [81771506, 31571410, 31570827], National Key R&D Program of China [2018YFA0107000], and Guangzhou Municipal People's Livelihood Science and Technology Plan [201803010108].

Author Contributions

Z. Y. and L. H. designed the study, analyzed data, and wrote the paper. L. H., X. Y., Z. Z., M. P., and L. J. performed majority of experiments. M. W. offered ideas and helped analyzing data. Z. Y. supervised the project. All authors read and approved the manuscript.

Declarations of Interest

None.

Appendix A. Supplementary Data

Supplementary data to this article can be found online at https://doi.org/10.1016/j.neo.2018.07.004.

References

[1] Cesare AJ and Reddel RR (2010). Alternative lengthening of telomeres: models, mechanisms and implications. *Nat Rev Genet* **11**, 319–330.
[2] Nabetani A and Ishikawa F (2011). Alternative lengthening of telomeres pathway: recombination-mediated telomere maintenance mechanism in human cells. *J Biochem* **149**, 5–14.
[3] Chung I, Osterwald S, Deeg KI, and Rippe K (2012). PML body meets telomere: the beginning of an ALTernate ending? *Nucleus* **3**, 263–275.
[4] Venturini L, Erdas R, Costa A, Gronchi A, Pilotti S, Zaffaroni N, and Daidone M (2008). ALT-associated promyelocytic leukaemia body (APB) detection as a reproducible tool to assess alternative lengthening of telomere stability in liposarcomas. *J Pathol* **214**, 410–414.
[5] Henson JD, Cao Y, Huschtscha LI, Chang AC, Au AY, Pickett HA, and Reddel RR (2009). DNA C-circles are specific and quantifiable markers of alternative-lengthening-of-telomeres activity. *Nat Biotechnol* **27**, 1181–1185.
[6] Cesare AJ and Griffith JD (2004). Telomeric DNA in ALT cells is characterized by free telomeric circles and heterogeneous t-loops. *Mol Cell Biol* **24**, 9948–9957.
[7] Dunham MA, Neumann AA, Fasching CL, and Reddel RR (2000). Telomere maintenance by recombination in human cells. *Nat Genet* **26**, 447–450.
[8] Londono-Vallejo JA, Der-Sarkissian H, Cazes L, Bacchetti S, and Reddel RR (2004). Alternative lengthening of telomeres is characterized by high rates of telomeric exchange. *Cancer Res* **64**, 2324–2327.
[9] Ciccia A and Elledge SJ (2010). The DNA damage response: making it safe to play with knives. *Mol Cell* **40**, 179–204.
[10] Nabetani A and Ishikawa F (2009). Unusual telomeric DNAs in human telomerase-negative immortalized cells. *Mol Cell Biol* **29**, 703–713.
[11] Lovejoy CA, Li W, Reisenweber S, Thongthip S, Bruno J, de Lange T, De S, Petrini JH, Sung PA, and Jasin M, et al (2012). Loss of ATRX, genome instability, and an altered DNA damage response are hallmarks of the alternative lengthening of telomeres pathway. *PLoS Genet* **8**e1002772.
[12] Nabetani A, Yokoyama O, and Ishikawa F (2004). Localization of hRad9, hHus1, hRad1, and hRad17 and caffeine-sensitive DNA replication at the alternative lengthening of telomeres-associated promyelocytic leukemia body. *J Biol Chem* **279**, 25849–25857.
[13] Cesare AJ, Kaul Z, Cohen SB, Napier CE, Pickett HA, Neumann AA, and Reddel RR (2009). Spontaneous occurrence of telomeric DNA damage response in the absence of chromosome fusions. *Nat Struct Mol Biol* **16**, 1244–1251.
[14] Mao P, Liu J, Zhang Z, Zhang H, Liu H, Gao S, Rong YS, and Zhao Y (2016). Homologous recombination-dependent repair of telomeric DSBs in proliferating human cells. *Nat Commun* **7**12154.
[15] Doksani Y and de Lange T (2016). Telomere-internal double-strand breaks are repaired by homologous recombination and PARP1/Lig3-dependent end-joining. *Cell Rep* **17**, 1646–1656.
[16] Cho NW, Dilley RL, Lampson MA, and Greenberg RA (2014). Interchromosomal homology searches drive directional ALT telomere movement and synapsis. *Cell* **159**, 108–121.
[17] Reddel RR, Bryan TM, and Murnane JP (1997). Immortalized cells with no detectable telomerase activity. A review. *Biochemistry (Mosc)* **62**, 1254–1262.
[18] Dilley RL, Verma P, Cho NW, Winters HD, Wondisford AR, and Greenberg RA (2016). Break-induced telomere synthesis underlies alternative telomere maintenance. *Nature* **539**, 54–58.
[19] Ouellette MM, Liao M, Herbert BS, Johnson M, Holt SE, Liss HS, Shay JW, and Wright WE (2000). Subsenescent telomere lengths in fibroblasts immortalized by limiting amounts of telomerase. *J Biol Chem* **275**, 10072–10076.
[20] Williams ES and Bailey SM (2009). Chromosome orientation fluorescence in situ hybridization (CO-FISH). *Cold Spring Harb Protoc* **4**, 1012–1017.
[21] Huang J, Wang F, Okuka M, Liu N, Ji G, Ye X, Zuo B, Li M, Liang P, and Ge WW, et al (2011). Association of telomere length with authentic pluripotency of ES/iPS cells. *Cell Res* **21**, 779–792.

[22] Kim NW, Piatyszek MA, Prowse KR, Harley CB, West MD, Ho PL, Coviello GM, Wright WE, Weinrich SL, and Shay JW (1994). Specific association of human telomerase activity with immortal cells and cancer. *Science* **266**, 2011–2015.

[23] Salic A and Mitchison TJ (2008). A chemical method for fast and sensitive detection of DNA synthesis in vivo. *Proc Natl Acad Sci U S A* **105**, 2415–2420.

[24] Bailey SM, Cornforth MN, Kurimasa A, Chen DJ, and Goodwin EH (2001). Strand-specific postreplicative processing of mammalian telomeres. *Science* **293**, 2462–2465.

[25] Kuo CF, Mol CD, Thayer MM, Cunningham RP, and Tainer JA (1994). Structure and function of the DNA repair enzyme exonuclease III from E. coli. *Ann N Y Acad Sci* **726**, 223–234 [discussion 234-225].

[26] Tong AS, Stern JL, Sfeir A, Kartawinata M, de Lange T, Zhu XD, and Bryan TM (2015). ATM and ATR signaling regulate the recruitment of human telomerase to telomeres. *Cell Rep* **13**, 1633–1646.

[27] Zhao Y, Abreu E, Kim J, Stadler G, Eskiocak U, Terns MP, Terns RM, Shay JW, and Wright WE (2011). Processive and distributive extension of human telomeres by telomerase under homeostatic and nonequilibrium conditions. *Mol Cell* **42**, 297–307.

[28] El Daly H and Martens UM (2007). Telomerase inhibition and telomere targeting in hematopoietic cancer cell lines with small non-nucleosidic synthetic compounds (BIBR1532). *Methods Mol Biol* **405**, 47–60.

[29] Anand RP, Lovett ST, and Haber JE (2013). Break-induced DNA replication. *Cold Spring Harb Perspect Biol* **5**, a010397.

[30] Bryan TM, Englezou A, Gupta J, Bacchetti S, and Reddel RR (1995). Telomere elongation in immortal human cells without detectable telomerase activity. *EMBO J* **14**, 4240–4248.

[31] Zhang T, Zhang Z, Li F, Hu Q, Liu H, Tang M, Ma W, Huang J, Songyang Z, and Rong Y, et al (2017). Looping-out mechanism for resolution of replicative stress at telomeres. *EMBO Rep* **8**, 1412–1428.

[32] Wu G, Jiang X, Lee WH, and Chen PL (2003). Assembly of functional ALT-associated promyelocytic leukemia bodies requires Nijmegen breakage syndrome 1. *Cancer Res* **63**, 2589–2595.

[33] Michel B, Flores MJ, Viguera E, Grompone G, Seigneur M, and Bidnenko V (2001). Rescue of arrested replication forks by homologous recombination. *Proc Natl Acad Sci U S A* **98**, 8181–8188.

[34] Branzei D and Szakal B (2016). DNA damage tolerance by recombination: molecular pathways and DNA structures. *DNA Repair (Amst)* **44**, 68–75.

[35] Flynn RL, Cox KE, Jeitany M, Wakimoto H, Bryll AR, Ganem NJ, Bersani F, Pineda JR, Suva ML, and Benes CH, et al (2015). Alternative lengthening of telomeres renders cancer cells hypersensitive to ATR inhibitors. *Science* **347**, 273–277.